Physics of Fluids

Capillary filling in drop merging: Dynamics of the four-phase contact point

Cite as: Phys. Fluids **34**, 012107 (2022); https://doi.org/10.1063/5.0073057
Submitted: 27 September 2021 • Accepted: 12 December 2021 • Published Online: 05 January 2022

Peyman Rostami and Günter K. Auernhammer

Physics of Fluids ARTICLE scitation.org/journal/phf

Capillary filling in drop merging: Dynamics of the four-phase contact point

Cite as: Phys. Fluids **34**, 012107 (2022); doi: 10.1063/5.0073057
Submitted: 27 September 2021 · Accepted: 12 December 2021 ·
Published Online: 5 January 2022

View Online Export Citation CrossMark

Peyman Rostami[a] and Günter K. Auernhammer[b]

AFFILIATIONS

Abteilung Polymergrenzflächen, Leibniz-Institut für Polymerforschung Dresden e.V., Hohe Str. 6, 01069 Dresden, Germany

[a]**Also at:** Max Planck Institute for Polymer Research, Physics at Interfaces, Ackermannweg 10, 55128 Mainz, Germany. **Electronic mail:** rostami@ipfdd.de
[b]**Author to whom correspondence should be addressed:** auernhammer@ipfdd.de

ABSTRACT

The merging of immiscible drops differs significantly from the merging of miscible drops due to the formation of a liquid–liquid interface between drops. The immiscibility requires the formation of a four-phase contact point, where the drops, the gas, and the substrate meet. We show that this point has its own unique dynamics, never studied beforehand. For very different scenarios, the propagation distance of this point follows scales with time like $t^{\frac{1}{2}}$. A model balancing the driving and dissipative forces agrees with our experiments.

INTRODUCTION

Drop merging plays an important role in industrial and natural phenomena from emulsions and microfluidics to printing technology and metallurgy.[1–4] Most of the early studies were performed with drops with identical liquids.[5–7] Later drops with different liquids are studied, and most of these works focus on early stages of coalescence.[8,9] Studies on dynamic wetting along liquid–liquid interfaces are rare, e.g., Refs. 10 and 11. In the drop merging, Marangoni tensions and the induced flow play essential roles[12,13] and can dominate this process. However, one important geometric feature of two non-identical drops on a substrate seems to be overlooked so far. In three dimensional space, n phases contact in an object with $4-n$ dimensions. When we consider two immiscible drops on a substrate in a gas phase, $n=4$, this implies that there is a contact point in which all four phases meet. Here, we show that this four-phase contact point (FPCP from now on) has its own dynamics, which has a characteristic timescale that differs significantly from other timescales.

The statics of the FPCP was introduced about two decades ago.[14] So far, the mechanical stability of specific configurations has been analyzed.[15–17] Another example of capillary wetting on liquid–liquid interfaces is drop encapsulation, where the liquid with lower surface tension surrounds the other drop. During this process, capillary force acts in the three phase contact line and leads to encapsulating the drop.[18] Despite its relevance for microfluidics,[19,20] etc., little work on drop merging of immiscible drops is done on solid surfaces.[21]

Capillarity driven filling in capillaries and V-shaped grooves is both a long studied problem and still an active field of research. This is due to the fact that passive capillary flow inside macro- and micro-channels is used in wide range of applications like microfluidics,[22,23] printing technologies,[24] capillary pumping,[25] or liquid imbibition in different scales.[26,27] More than three centuries ago, Hauksbee and Jurin published first accounts on the static shape of a water meniscus in the wedge between two touching glass plates.[28–30] Lucas[31] and Washburn[32] studied independently the dynamic filling of capillaries by solving the hydrodynamic problem inside the capillary, i.e., the force balance between driving and dissipating forces. For zero gravity condition, e.g., a horizontal capillary, only the capillary driving force and viscous dissipation force are relevant. By writing this force balance, it can be shown that the penetration length H inside the capillary scales with the square root of time, Eq. (1). The coefficient of penetration D combines the radius of the capillary r, the cosine of contact angle θ, and the ratio of surface tension γ to viscosity of liquid η,

$$H^2(t) = \frac{\gamma}{\eta}\frac{\cos(\theta)}{2} rt \equiv D^2 t. \tag{1}$$

It has been shown that the structure of this solution can be used for tubes of different cross sections on different length scales.[33–38] The same scaling with time also applies for the propagation of liquid in open micro-channels.[36,39,40] In these cases, the coefficient of penetration picks up geometry parameters of the channel. A typical example

is capillary flow inside an open V-shaped channel that was studied numerically[41] and experimentally.[37,39,42] Recently, the capillary filling inside an open micro-channel, which is already filled with another immiscible liquid,[43] was studied, which again follows the Washburn scaling $H^2 \sim t$.

In this study, we go beyond these established scenarios. We follow the merging dynamics of immiscible drops that initially touch along the contact line. We find that there is a unique dynamics of the FPCP that decouples from the rest of the merging dynamics of the drops. The lower surface tension of liquid engulfs the higher surface tension drop along the contact line of the drop, see Fig. 1(b). The propagation of the FPCP has strong similarities to capillary filling phenomena as described by the Lucas–Washburn equation, Eq. (1), and follows the same scaling. To demonstrate this scaling, we systematically vary parameters: (i) the ratio of surface tension to viscosity of second drop, (ii) the viscosity of pre-deposited first drop, and (iii) the wetting properties of the substrate. These parameter variations allow us to develop and test a simple analytical model that describes the dynamics of the FPCP.

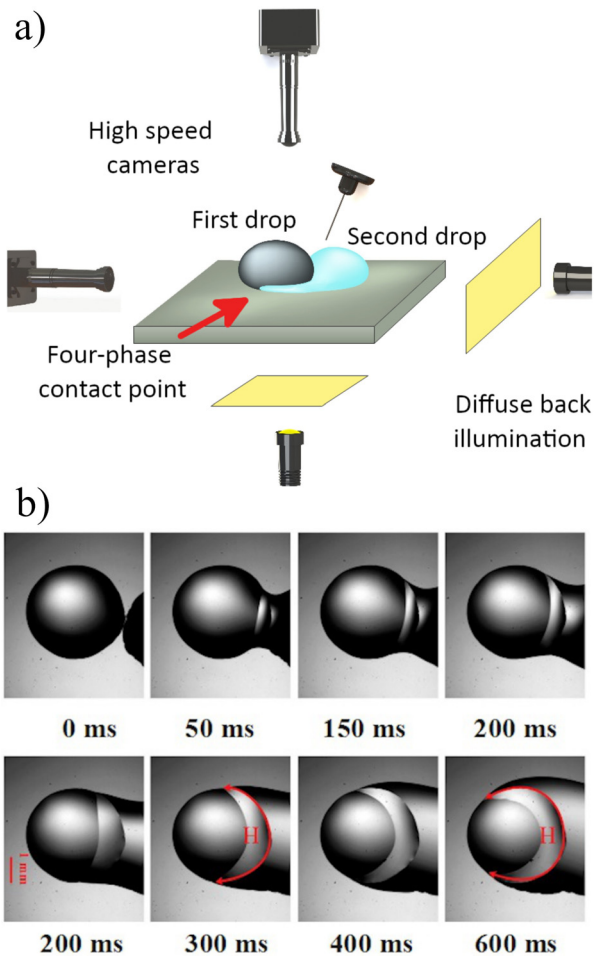

FIG. 1. (a) Sketch of the setup with an illustration of the FPCP. (b) Time series in top view of drop merging when the first drop (left, here water) is already deposited and the second drop (bromocycloheptane) comes to contact, the FPCP position is highlighted by arrows. H measures the length of the contact line of the first drop that is wetted by the second drop.

METHODS AND MATERIALS

We follow the drop merging with two high-speed cameras, having orthogonal directions of observation, see Fig. 1(a). The drops are deposited on a glass substrate with syringes pumps. We place the drops far apart each other to prevent the effect of gravity or inertia of the second drop. The two drops come to contact to each other with spreading velocity in the range of few millimeter per second of the second drop. In all experiments, the ratio of the volumes of the first and second drops is ≈1. The cameras are equipped with Navitar objectives with a maximum 12× magnification with a 2× F-mount adapter, allowing for a lateral size of the field of view of 17.5 mm) at a frame rate of 1000 Hz. Two light emitting diode (LED) lamps with diffuser sheets provide a uniform illumination of the observation section. All the experimental results are obtained under controlled environmental conditions with a relative humidity 48 ± 3% and a temperature 23.0 ± 0.5 °C. Glass substrates are cleaned before performing the experiments.

We use two classes of liquids: High surface tension liquids (water, glycerin, and mixtures thereof) and brominated oils as low surface tension liquids. At the experimental timescales analyzed in this work, the brominated oils are immiscible in the polar liquids to a good approximation. When two immiscible drops with different surface tensions coalescence, the drop with lower surface tension surrounds the drop with high surface tension to minimize the surface energy. The final stages of this process are also discussed in Refs. 14–17. The purchased chemicals are used as delivered without further purification. For particle tracking experiments, polystyrene particles are used. The physical properties of the used liquids are listed in Table I. Further details on the materials and the experimental procedure are given in the supplementary material.

DYNAMICS OF THE FOUR PHASE CONTACT POINT

In all experiments, at contact of the two drops, two FPCPs form at both sides of the neck, where the two liquids, the substrate, and the gas phase meet, see Fig. 1(b). The propagating FPCPs "wet" the contact line of the first drop. The length of this "wetted" contact line is the called H. Along this length the liquid–gas–solid contact line is changed into a liquid–liquid–solid contact line. This change actually leaves the position of the contact line of the first drop on the substrate almost unchanged. These FPCPs travel around the first drop and annihilate

TABLE I. Physical properties of liquids. Water, glycerin, and mixtures, thereof, were used as liquids for the first drops. The other liquids were used for the second drops.

Chemicals	Surface tension (mN/m)	Viscosity (mPa·s)	Surface tension to viscosity (m/s)
Water	72.1 ± 0.1	0.9321[44]	80.1
Glycrine	63.5 ± 0.1	1078[45,46]	0.06
Bromocyclopentane	33.2 ± 0.1	1.4 ± 0.05	23.7
Bromocyclohexane	32.1 ± 0.1	2.2 ± 0.05	14.6
Bromocycloheptane	31.5 ± 0.1	3.9 ± 0.05	8.1

each other when contacting at the other side of the first drop. A quantitative analysis shows that the advancing FPCP propagates with a power law $H(t) \sim t^{\frac{1}{2}}$, see Fig. 2(c).

The cross-sectional area filled by the second drop near the FPCP is illustrated in Fig. 2(a), along with the similarity to the filling of a V-shaped groove, see Fig. 2(b). The propagating liquid (blue) is confined between a solid, the glass substrate, and the liquid–liquid interface to first drop. Despite the similarities, there is an important difference. The classical Washburn case considers solid walls, but in our case, one boundary of the "groove" is the liquid of the first drop. This liquid–liquid interface can deform and exhibits a different hydrodynamic boundary condition for the flow of the second drop. However, still, the FPCP follows the general Washburn scaling $H(t) \sim t^{\frac{1}{2}}$. Can we apply the Washburn modeling to the present case? If yes, how much it will deviate from general phenomena because of the liquid wall and dynamic time-dependent geometry? To approach these questions, several key mechanisms have to be checked, including the ratio between surface tension and viscosity and the viscosity and contact angle of the first drop.

The similarity of the dynamic spreading in a groove and the classical Washburn case was shown previously.[37,47] Romero and Yost[37] developed a quantitative model. Since this model uses one fluid and assumes solid walls, we call it the "one fluid model." In this model, the coefficient of penetration D contains two contributions: (i) the ratio of the surface tension and the viscosity γ/η multiplied with a typical lateral dimension of the channel (here its depth l_0), and (ii) a geometric factor $K(\alpha, \theta)$ that depends on the contact angle and the opening angle of the V-shaped groove,

$$H^2(t) = K(\alpha, \theta)\frac{\gamma l_0}{\eta}t, \tag{2}$$

where

$$K(\alpha, \theta) = \frac{1}{2\pi \sin(\alpha)}\left[\cos(\theta) - \frac{(\alpha - \theta)\cos(\alpha)}{\sin(\alpha - \theta)}\right]. \tag{3}$$

For a systematic variation of the ratio (γ/η) in the spreading drop, we use liquids that are chemically very similar, with approximately the same surface tension, but different viscosities, see Table I. For all liquids combinations, the length H of the wetted contact line is proportional to the square root of time. By increasing the ratio of surface tension to viscosity, the FPCP travels faster, i.e., the coefficient of penetration is increasing, see Fig. 3(a). There is, however, a

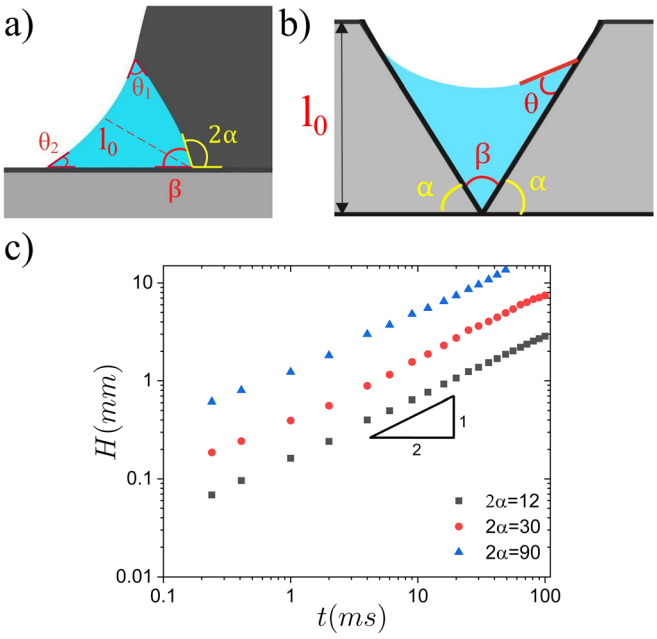

FIG. 2. (a) The cross section near the FPCP illustrates the similarity to the V-groove. The FPCP propagates perpendicular to this cross-sectional plane. (b) Schematic of V-groove channel: depth of channel (l_0), contact angle of the filling liquid with the walls (θ), opening angle of groove (β), and the angle between wall and horizontal line (α). It should be mentioned that in both cases; ($2\alpha + \beta = 180°$). The FPCP propagates perpendicular to this cross-sectional plane. (c) Typical dynamics of the FPCP. Here, for the liquid pair of water (first drop) and bromocyclohexane (second drop) on substrates with different hydrophobicity, as indicated by the contact angle of water (α).

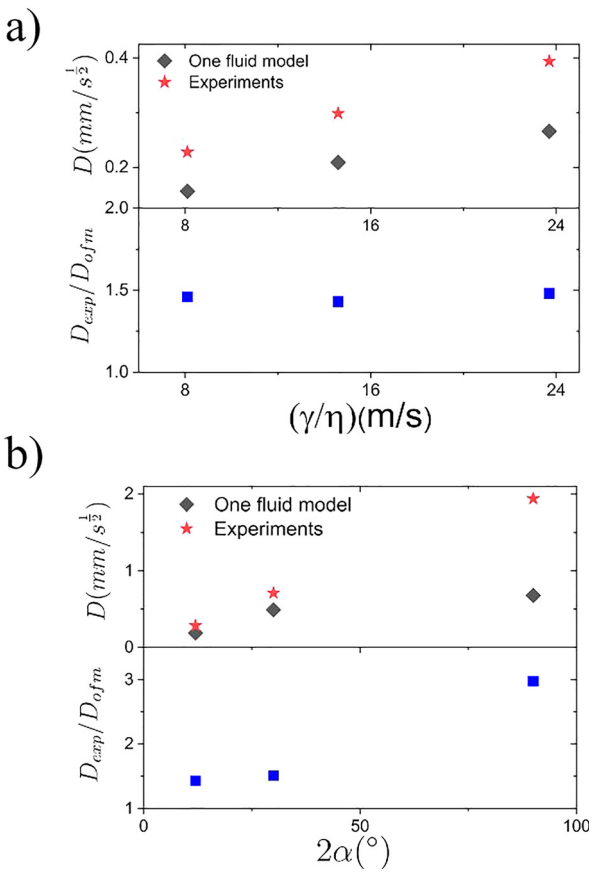

FIG. 3. (a) The coefficient of penetration as measured experimentally D_{exp} and according to the one fluid model, Eq. (2), D_{ofm}, using the data given in Table I. In all cases, water is used as first drop. The ratio D_{exp}/D_{ofm} is plotted below the graph. (b) The coefficient of penetration as measured experimentally D_{exp} and according to the one fluid model, Eq. (2), D_{ofm} for water (first drop) and bromocyclohexane (second drop) on substrates with different hydrophobicity, as indicated by the contact angle of water (2α).

pronounced difference between the experimental data and the predictions of the one fluid model, even when taking the drop height of the first drop as an upper bound of the groove depth l_0. All experiments for this section are done on the cleaned hydrophilic substrate, which means that the apparent contact angle of all the first drops is around 15°.

A similar systematic difference is observed when changing the opening angle of groove β, see Fig. 3(b). We use surface modifications to change the contact angles. Obviously, this changes the contact angles of both drops. Thus, a surface modification changes the opening angle of the groove β and the drop height [Fig. 2(a)]. The one fluid model, Eq. (2), predicts that the dynamics of the FPCP speeds up when the opening angle of groove (β) decreases, i.e., for higher contact angles of the first drop. Experimentally, the FPCP propagates significantly faster for more hydrophobic surfaces. In these experiments, we used the different hydrophobicity of the substrate to achieve different contact angles: 15°, 30°, and 90° depending on the surface modification. The ratio of D_{exp}/D_{ofm} remains constant as a function of the surface tension to viscosity ratio. On the other hand, this ratio increases rapidly by increasing the apparent contact angle.

The coefficient of penetration shows qualitatively in the right trend on γ/η and the opening angle of the groove. However, the one fluid model systematically underestimates the dynamics of the FPCP (Fig. 3). Potential reasons for this difference are: (i) The capillary driving originates from two different surfaces, the liquid–solid interface, and the liquid–liquid interface. The unbalanced capillary force that drives spreading differs on these two interfaces. Additionally, the contact between the two liquid induces Marangoni tensions that can induce flow in the first drop.[13] (ii) The geometry changes during the spreading of the second drop, because the first drop deforms during the spreading process. (iii) The hydrodynamic boundary condition at the liquid–liquid interface differs from the one on the substrate and depends on the viscosity ratio of the two liquids. (iv) The contact angles depend on contact line velocity, which might scale with the velocity of FPCP.[48] All these effects only influence the prefactor K but do not change the basic scaling with time $H \sim t^{\frac{1}{2}}$. The capillary driving and the viscous dissipation are localized in a narrow region close to the moving contact lines. Consequently, a small region close to the FPCP should dominant for its dynamics.

MODEL THE FOUR PHASE CONTACT POINT DYNAMICS

In the capillary rise problem, inertia only plays a minor role and can be neglected in many cases. For this reason, we assume that inertia can also be neglected in a first approximation and the FPCP dynamic is a viscous flow, which follows the Poiseuille flow assumption.[49]

The general case of filling of groove was solved by Yost and coworkers.[37] In this solution, the authors argue that the scaling of $H \sim \sqrt{t}$ is rather general and applies also for the tip of the wetting liquid in a partially filled V-shaped groove. They show that the final result is the same as given in Eq. (2). The geometrical differences between horizontal tubes and grooves can be covered by a prefactor to the scaling. Due to this equivalence and for sake of simplicity, we adopt the presented approach,[39] knowing that the scaling also applies for partially filled grooves. The tip of the wetting liquid as calculated by Yost and coworkers[37,39] corresponds to the FPCP in our case.

To capture the basic differences mentioned above, for the liquid wall, we consider a multiphase flow with a geometry of concentric cylinders, where the boundary between the inner and outer cylinder is assumed radially undeformable [Fig. 4(b)]. This outer cylinder mimics the first drop (region 1), the inner cylinder the second drop (region 2). The dynamics of capillary flow inside a tube can be written by the force balance between driving mechanisms and dissipation forces.[39] We give details of the calculation in the supplementary material,

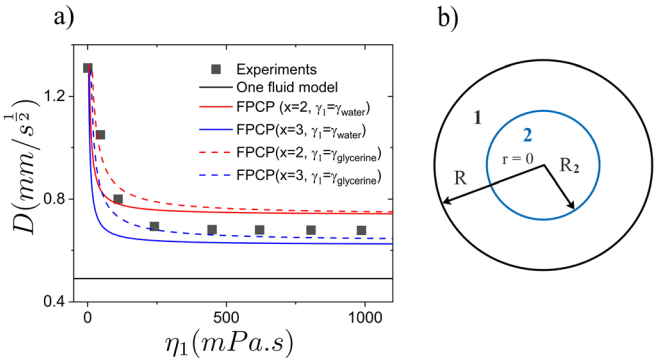

FIG. 4. (a) Coefficient of penetration as the function of first drop viscosity with bromocyclohexane as the second drop. The experimental results are compared with one fluid model and four phase contact point model with different x values. (b) Schematic for the modeling of the flow with two fluids inside the cylinder, the inner region is assumed as filling liquid or second drop and outer section is the first drop. (R_2 and R are the radii of inner and outer regions.)

$$H(t) = \sqrt{\frac{l_0 K(\gamma, \alpha, \theta_1, \theta_2)}{4\pi\eta_{\mathrm{eff}}}}\, t. \tag{4}$$

Here, we introduced an effective viscosity η_{eff}, a modified geometric factor $K(\gamma, \alpha, \theta_1, \theta_2)$, Eq. (S10), and the ratio of the outer and inner radius $x = R/R_2 \geq 1$, see Fig. 4,

$$\eta_{\mathrm{eff}} = \frac{1}{2}\left(\eta_2 + \frac{\eta_1\eta_2}{\eta_1 + 2\eta_2(x^2-1)}\right). \tag{5}$$

This model depends only weakly on the value of x. $2 \leq x \leq 4$ are compatible with our data, see also Fig. S2. However, the results remain in the same range for higher value of x; we consider two cases of $x = 2$ and $x = 3$.

Increasing the viscosity of the pre-deposited first drop allows for a simple test of the crossover between a liquid (low viscous) and a quasi-solid (highly viscous) wall. Since the additives for changing the viscosity typically also change the surface tensions, the driving force is indirectly a weak function of the viscosity. This weak dependence has, however, no significant influence on the quality of the model comparison [compare Fig. 4(a)]. Increasing the viscosity of the pre-deposited first drop also increases η_{eff}. Consequently, the viscous force F_η increases, and the filing rate decreases, see Eq. (4).

To illustrate this, we compare the merging of bromocyclohexane drop with different pre-deposited drops of water, glycerin, and mixtures thereof (Fig. 4). The apparent contact angle of all the first drops stays in the range $25° \leq 2\alpha \leq 30°$. The surface tension differences of the liquid pairs are also close, $33\,\mathrm{mNm}^{-1} \leq \gamma_1 - \gamma_2 \leq 28\,\mathrm{mNm}^{-1}$. Consequently, the driving forces vary by less than 20%. In contrast, the coefficient of penetration reduces by 50%.

Experimentally, the coefficient of penetration only depends on the viscosity of the first drop for small enough viscosities (Fig. 4).

For the first drop viscosity $\eta_1 \gtrsim 250$, the coefficient of penetration remains constant. Increasing the viscosity is almost equivalent to the shift from a liquid–liquid interface at one of the walls and to liquid–-quasi solid interface. The one fluid model does not cover this viscosity dependence (Fig. 4). In contrast, our model above gives a good description of the behavior. Despite the simplifications in our model and the omitted dynamic effects, the difference between our model and the experimental data is below 10% for D.

Our model of the dynamics of the FPCP is in almost quantitative agreement with the experimental data. The remaining differences between our model and experiments can be explained by several facts. Probably other forces play a role that were neglected in the present model, i.e., Marangoni stress between the two liquids. Additionally, the FPCP is highly dynamic and the geometry of the wedge changes during the experiments. Obviously, neglecting these effects does not seem to influence the dynamics of the FPCP significantly. To show the generality of our model, another pair of liquids is investigated: the fluorinated oil HFE7200 and pure glycerin. The results reveal two points; first with very different liquids again, the FPCF follows the square root of time. Second, our model can predict the flow with a reasonable accuracy. The details are included in the supplementary material, Fig. S4 and discussion thereof.

CONCLUSION

In this contribution, we have investigated the dynamics of the FPCP (four-phase contact point), where two liquids, the substrate, and the gas phase are in contact. During drop merging, this FPCP shows a dynamics that is independent of other processes like contact line velocity. The dynamics of this point follows the same scaling as the capillary flow inside the tube as originally described by Lucas and Washburn. The motion of the FPCP is consistent with $H(t) \approx Dt^{\frac{1}{2}}$ for all investigated cases, with the coefficient of penetration D. The geometry of the moving FPCP resembles the spreading of liquid in a V-shape groove, of which the dynamics can be reduced to the Lucas–Washburn case. Different to the classical case of the V-shape grooves, in the present case, one of the "walls" of the groove is liquid, i.e., the pre-deposited first drop. Despite this deformable boundary and the other differences to the classical case, the governing mechanisms are the same. Various material and geometry parameters can be included in a simple model that describes the dynamics of the FPCP almost quantitatively.

The FPCP, which is introduced here, not only reveals a unique dynamic but also leads to higher mobility of the liquid. Since we substitute, one solid wall with a liquid wall higher mobility is expected and it can lead to higher efficiency of systems. These new phenomena should be relevant in microfluidics, patterned coating, and printing technology.

SUPPLEMENTARY MATERIAL

See the supplementary material for details of additional information on methods and materials; the derivation of the four-phase contact point model and its theoretical calculation; and additional information on time dependence of four-phase contact point and contact line velocity.

ACKNOWLEDGMENTS

This study was funded by the German Research Foundation (DFG) within the Collaborative Research Centre 1194 "Interaction between Transport and Wetting Processes," Project-ID No. 265191195, Subproject Nos. A02 (P.R.) and A06 (G.K.A.). In addition, the authors wish to thank Benedikt Straub and Stefan Michel for fruitful discussion.

AUTHOR DECLARATIONS

Conflict of Interest

The authors have no conflicts of interest to disclose.

DATA AVAILABILITY

The data that support the findings of this study are available from the corresponding author upon reasonable request.

REFERENCES

[1]H. Gu, M. H. Duits, and F. Mugele, "Droplets formation and merging in two-phase flow microfluidics," Int. J. Mol. Sci. **12**, 2572–2597 (2011).
[2]V. Varma, A. Ray, Z. Wang, Z. Wang, and R. Ramanujan, "Droplet merging on a lab-on-a-chip platform by uniform magnetic fields," Sci. Rep. **6**, 37671 (2016).
[3]A. D. Graham, S. N. Olof, M. J. Burke, J. P. Armstrong, E. A. Mikhailova, J. G. Nicholson, S. J. Box, F. G. Szele, A. W. Perriman, and H. Bayley, "High-resolution patterned cellular constructs by droplet-based 3D printing," Sci. Rep. **7**, 7004 (2017).
[4]E. Antonopoulou, O. Harlen, M. Rump, T. Segers, and M. Walkley, "Effect of surfactants on jet break-up in drop-on-demand inkjet printing," Phys. Fluids **33**, 072112 (2021).
[5]G. Charles and S. Mason, "The coalescence of liquid drops with flat liquid/liquid interfaces," J. Colloid Sci. **15**, 236–267 (1960).
[6]W. Ristenpart, P. McCalla, R. Roy, and H. Stone, "Coalescence of spreading droplets on a wettable substrate," Phys. Rev. Lett. **97**, 064501 (2006).
[7]J. Sun, B. Bao, M. He, H. Zhou, and Y. Song, "Recent advances in controlling the depositing morphologies of inkjet droplets," ACS Appl. Mater. Interfaces **7**, 28086–28099 (2015).
[8]S. Karpitschka and H. Riegler, "Noncoalescence of sessile drops from different but miscible liquids: Hydrodynamic analysis of the twin drop contour as a self-stabilizing traveling wave," Phys. Rev. Lett. **109**, 066103 (2012).
[9]M. A. Bruning, M. Costalonga, S. Karpitschka, and J. H. Snoeijer, "Delayed coalescence of surfactant containing sessile droplets," Phys. Rev. Fluids **3**, 073605 (2018).
[10]M. Reddy, M. Manivannan, M. G. Basavaraj, and S. P. Thampi, "Statics and dynamics of drops spreading on a liquid-liquid interface," Phys. Rev. Fluids **5**, 104006 (2020).
[11]M. A. Hack, W. Tewes, Q. Xie, C. Datt, K. Harth, J. Harting, and J. H. Snoeijer, "Self-similar liquid lens coalescence," Phys. Rev. Lett. **124**, 194502 (2020).
[12]S. Karpitschka and H. Riegler, "Sharp transition between coalescence and non-coalescence of sessile drops," J. Fluid Mech. **743**, R1 (2014).
[13]P. Rostami, B. B. Straub, and G. K. Auernhammer, "Gas-phase induced Marangoni flow causes unstable drop merging," Langmuir **36**, 28–36 (2020).
[14]L. Mahadevan, M. Adda-Bedia, and Y. Pomeau, "Four-phase merging in sessile compound drops," J. Fluid Mech. **451**, 411 (2002).
[15]A. Ayyad and F. Aqra, "Mechanical stability of two immiscible liquid drops resting on a solid substrate," Phys. Chem. Liq. **49**, 430–434 (2011).
[16]Y. Zhang, D. Chatain, S. L. Anna, and S. Garoff, "Stability of a compound sessile drop at the axisymmetric configuration," J. Colloid Interface Sci. **462**, 88–99 (2016).
[17]C.-Y. Zhang, P. Gao, E.-Q. Li, and H. Ding, "On the compound sessile drops: Configuration boundaries and transitions," J. Fluid Mech. **917**, A37 (2021).
[18]R. B. Koldeweij, B. F. Van Capelleveen, D. Lohse, and C. W. Visser, "Marangoni-driven spreading of miscible liquids in the binary pendant drop geometry," Soft Matter **15**, 8525–8531 (2019).
[19]P. Dunne, T. Adachi, A. A. Dev, A. Sorrenti, L. Giacchetti, A. Bonnin, C. Bourdon, P. H. Mangin, J. M. D. Coey, B. Doudin, and T. M. Hermans, "Liquid flow and control without solid walls," Nature **581**, 58–62 (2020).
[20]F. Shen, Y. Li, Z. Liu, and X. Li, "Study of flow behaviors of droplet merging and splitting in microchannels using Micro-PIV measurement," Microfluid. Nanofluid. **21**, 66 (2017).

[21]T. Li, J. Li, L. Wang, Y. Duan, and H. Li, "Coalescence of immiscible liquid metal drop on graphene," Sci. Rep. **6**, 34074 (2016).
[22]K. W. Oh, K. Lee, B. Ahn, and E. P. Furlani, "Design of pressure-driven microfluidic networks using electric circuit analogy," Lab Chip **12**, 515–545 (2012).
[23]R. Seemann, M. Brinkmann, E. J. Kramer, F. F. Lange, and R. Lipowsky, "Wetting morphologies at microstructured surfaces," Proc. Natl. Acad. Sci. U. S. A. **102**, 1848 (2005).
[24]Q. Huang and Y. Zhu, "Gravure printing of water-based silver nanowire ink on plastic substrate for flexible electronics," Sci. Rep. **8**, 15167 (2018).
[25]W. Guo, J. Hansson, and W. van der Wijngaart, "Capillary pumping independent of the liquid surface energy and viscosity," Microsyst. Nanoeng. **4**(1), 7 (2018).
[26]C.-H. Tu, J. Zhou, M. Doi, H.-J. Butt, and G. Floudas, "Interfacial interactions during in situ polymer imbibition in nanopores," Phys. Rev. Lett. **125**, 127802 (2020).
[27]D. Seo, A. M. Schrader, S.-Y. Chen, Y. Kaufman, T. R. Cristiani, S. H. Page, P. H. Koenig, Y. Gizaw, D. W. Lee, and J. N. Israelachvili, "Rates of cavity filling by liquids," Proc. Natl. Acad. Sci. U. S. A. **115**, 8070 (2018).
[28]F. Hauksbee, "An account of an experiment touching the ascent of water between two glass planes," Philos. Trans. (1683–1775) **27**, 539–540 (1710).
[29]F. Hauksbee, "An account of an experiment touching the direction of a drop of oil of oranges, between two glass planes, towards any side of them that is nearest press'd together," Philosoph. Trans. (1683–1775) **27**, 395–396 (1710).
[30]J. Jurin, "II. An account of some new experiments, relating to the action of glass tubes upon water and quicksilver," Philosoph. Trans. (1683–1775) **30**, 1083–1096 (1717).
[31]R. Lucas, "Ueber das Zeitgesetz des kapillaren Aufstiegs von Flüssigkeiten," Kolloid-Z. **23**, 15–22 (1918).
[32]E. W. Washburn, "The dynamics of capillary flow," Phys. Rev. **17**, 273–283 (1921).
[33]L. Mammen, P. Papadopoulos, K. Friedemann, S. Wanka, D. Crespy, D. Vollmer, and H.-J. Butt, "Transparent and airtight silica nano- and microchannels with uniform tubular cross-section," Soft Matter **9**, 9824–9832 (2013).
[34]P. Wu, H. Zhang, A. Nikolov, and D. Wasan, "Rise of the main meniscus in rectangular capillaries: Experiments and modeling," J. Colloid Interface Sci. **461**, 195–202 (2016).
[35]Y. Liu, A. Hansen, E. Block, N. R. Morrow, J. Squier, and J. Oakey, "Two-phase displacements in microchannels of triangular cross-section," J. Colloid Interface Sci. **507**, 234–241 (2017).
[36]F. F. Ouali, G. McHale, H. Javed, C. Trabi, N. J. Shirtcliffe, and M. I. Newton, "Wetting considerations in capillary rise and imbibition in closed square tubes and open rectangular cross-section channels," Microfluid. Nanofluid. **15**, 309–326 (2013).
[37]L. A. Romero and F. G. Yost, "Flow in an open channel capillary," J. Fluid Mech. **322**, 109–129 (1996).
[38]T. Ohzono, H. Monobe, K. Shiokawa, M. Fujiwara, and Y. Shimizu, "Shaping liquid on a micrometre scale using microwrinkles as deformable open channel capillaries," Soft Matter **5**, 4658–4664 (2009).
[39]R. R. Rye, J. A. Mann, and F. G. Yost, "The flow of liquids in surface grooves," Langmuir **12**, 555–565 (1996).
[40]R. K. Lade, E. J. Hippchen, C. W. Macosko, and L. F. Francis, "Dynamics of capillary-driven flow in 3D printed open microchannels," Langmuir **33**, 2949–2964 (2017).
[41]I. Catton and G. R. Stroes, "A semi-analytical model to predict the capillary limit of heated inclined triangular capillary grooves," J. Heat Transfer **124**, 162–168 (2002).
[42]J. Tian, D. Kannangara, X. Li, and W. Shen, "Capillary driven low-cost V-groove microfluidic device with high sample transport efficiency," Lab Chip **10**, 2258–2264 (2010).
[43]D. Yang, M. Krasowska, C. Priest, M. N. Popescu, and J. Ralston, "Dynamics of capillary-driven flow in open microchannels," J. Phys. Chem. C **115**, 18761–18769 (2011).
[44]See https://wiki.anton-paar.com/en/water/ for "Viscosity of Water."
[45]See http://www.met.reading.ac.uk/~sws04cdw/viscosity_calc.html for "Calculate Density and Viscosity of Glycerol/Water Mixtures."
[46]N.-S. Cheng, "Formula for the viscosity of a glycerol–water mixture," Ind. Eng. Chem. Res. **47**, 3285–3288 (2008).
[47]R. Lenormand and C. Zarcone, "Role of roughness and edges during imbibition in square capillaries," presented at the SPE Annual Technical Conference and Exhibition, Houston, TX, 16–19 September 1984, Paper No. SPE-13264-MS.
[48]J. H. Snoeijer and B. Andreotti, "Moving contact lines: Scales, regimes, and dynamical transitions," Annu. Rev. Fluid Mech. **45**, 269–292 (2013).
[49]J. Kim, M.-W. Moon, and H.-Y. Kim, "Capillary rise in superhydrophilic rough channels," Phys. Fluids **32**, 032105 (2020).